Review Article

The role of virtual photons in nanoscale photonics

David L. Andrews* and David S. Bradshaw

The fundamental theory of processes and properties associated with nanoscale photonics should properly account for the quantum nature of both the matter and the radiation field. A familiar example is the Casimir force, whose significant role in nanoelectromechanical systems is widely recognised; the correct representation invokes the creation of short-lived virtual photons from the vacuum. In fact, there is an extensive range of nanophotonic interactions in which virtual photon exchange plays a vital role, mediating the coupling between particles. This review surveys recent theory and applications, also exhibiting novel insights into key electrodynamic mechanisms. Examples are numerous and include: laser-induced inter-particle forces known as optical binding; non-parametric frequency-conversion processes especially in rare-earth doped materials; light-harvesting polymer materials that involve electronic energy transfer between their constituent chromophores. An assessment of these and the latest prospective applications concludes with a view on future directions of research.

1 Introduction

A virtual photon can most simply be described as light that passes between two particles of matter without explicit measurement of its properties. This definition is one that provides a good working basis for describing interactions on the nanoscale, which is where the most distinctive features of 'virtuality' are exhibited. Virtual photon coupling pervades and underpins the theory behind a surprisingly large range of phenomena, most notably in the mechanisms for electrodynamic interactions over nanodimensions. It is a facet that is unfamiliar to many practitioners in this area, especially those whose interests are primarily experimental. Indeed, it will surprise many to find that a concept first introduced in the realm of elementary particle physics has a role to play in seemingly very remote areas of science – yet such features

have become increasingly evident, especially since the development of quantum electrodynamics (QED).

The concept of virtual photon exchange was originally introduced in quantum electrodynamical theory to describe non-contact couplings between charges, as for example electron-electron scattering. It is a hallmark of QED that such interactions are commonly represented by Feynman diagrams, as shown in Fig. 1(a). The physical origins of virtual photons have close connections to the 'vacuum fluctuations', which relate to the QED insight that every radiation mode has a finite (non-zero) ground state energy [1]. Accordingly, background (or zero point) energy is ever present, even when photons seemingly are not: the whole of space is pervaded by lowest-energy quantum electromagnetic fields associated with this energy. However, virtual photons are transient fluctuations that derive from the vacuum, existing in the form of a quantum excitation and then relaxation of the underlying quantum field. Photons of this type propagate unobserved over nanoscale dimensions with correspondingly large quantum uncertainties in energy and position. In some disciplines such as particle physics, the term *virtual photon cloud* has emerged as a vivid descriptor of how such photons emerge from, and retreat into, the space surrounding each material particle. It then becomes evident that it is the overlap of these clouds that leads to electromagnetic coupling: an analogy can be drawn with the overlap of atomic orbitals leading to chemical bonding. For example, the cohesion of matter in the condensed phase, through London attractive forces, is entirely attributable to virtual photon exchange.

When virtual photons are not recaptured in the immediate vicinity of their birthplace, their propagation characteristics acquire an increasingly real character, so that energy and momentum conservation become increasingly tight constraints. To a degree, the distinction between 'real' and 'virtual' photons can then be

* Corresponding author E-mail: david.andrews@physics.org
School of Chemistry, University of East Anglia, Norwich Research Park, Norwich, NR4 7TJ, United Kingdom
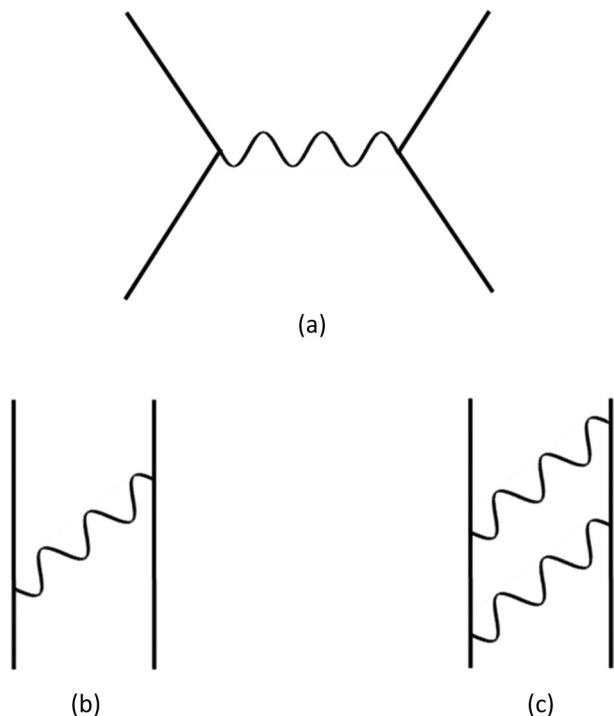
Wiley Online Library

Figure 1 Feynman diagrams (with time progressing upwards) representative of: (a) electron-electron scattering; (b) dipole-dipole coupling; (c) dispersion interactions. Wavy lines denote photons and the vertical lines, two nanoparticles. In contrast to the latter, the electrons in (a) are displayed as non-vertical lines since they are much smaller than nanoparticles and move at relativistic velocities (so cannot be assumed to remain in a fixed position during light-matter events).

considered a moot point. Although this, too, remains relatively unknown, the illusory (or at best, largely semantic) nature of this difference has been pointed out by many – for example one of the standard textbooks on elementary particle physics asserts that in some sense, every photon is virtual, as it is emitted and then sooner or later absorbed [2].

Each of these facets of virtual photon behaviour is drawn out in the account that follows. After Sec. 2, in which the formal theoretical basis of virtual photons is concisely laid out, Sec. 3 addresses the role in nanomechanical coupling, Sec. 4 examines applications in nonlinear optics, and Sec. 5 details electronic energy transfer processes and leads to the Conclusion.

2 Theoretical basis of virtual photons

In contrast to classical electromagnetism, where radiation is treated as waves and charged particles are influ-

enced by fields determined from Maxwell's equations, both radiation and particles are quantized in a quantum electrodynamical framework [3–8]. Although we note that the final result presented in this section is reproducible from a classical electrodynamical outlook [9, 10], in which instantaneous Coulombic interaction are supplemented with retardation effects associated with 'real' electromagnetic fields, it is the more rigorous QED formalism that better represents the underlying physics. In non-relativistic QED, the Hamiltonian of a scheme comprising particles labelled ξ is promoted to operator status, H, and is expressible in the multipolar form as:

$$H = \sum_{\xi} H_{\text{part}}(\xi) + \sum_{\xi} H_{\text{int}}(\xi) + H_{\text{rad}}, \qquad (1)$$

where H_{part} is the particle Hamiltonian, H_{rad} is the radiation Hamiltonian and H_{int} is the Hamiltonian representing the interaction of the radiation field with the particle. The H_{int} acts as a perturbation to the eigenstates of H_{part} and H_{rad}, conveniently providing for the quantum state of the system to be separated into particle and radiation states. By inspection of Eq. (1), contrasting with classical descriptions, it is clear that direct, instantaneous interactions between particles do not occur, *i.e.* interparticle couplings are mediated by the quantized electromagnetic field composed of virtual photons.

In the electric-dipole approximation, $H_{\text{int}}(\xi)$ is given by:

$$H_{\text{int}}(\xi) = -\sum_{\xi} \mu(\xi) \cdot e^{\perp}(\mathbf{R}_{\xi}). \qquad (2)$$

Here, the electric-dipole moment operator, $\mu(\xi)$, acts on particle states and the transverse electric field operator, $e^{\perp}(\mathbf{R}_{\xi})$, acts on radiation states. Since the electric field operator is identified with virtual photons, the explicit expression for $e^{\perp}(\mathbf{R}_{\xi})$ involves a summation over all virtual photon possibilities (*i.e.* all wave-vectors and polarizations). The quantum amplitude M_{FI}, the modulus square of which denotes the rate or efficiency of the given process, represents a coupling between any given initial system state $|I\rangle$ and final state $|F\rangle$, and is generally determined from time-dependent perturbation theory [11], so that:

$$M_{FI} = \langle F| \, H_{\text{int}} + H_{\text{int}} T_0 H_{\text{int}} + H_{\text{int}} T_0 H_{\text{int}} T_0 H_{\text{int}}$$
$$+ H_{\text{int}} T_0 H_{\text{int}} T_0 H_{\text{int}} T_0 H_{\text{int}} + ... \, |I\rangle, \qquad (3)$$

where successive terms relate to processes of progressively higher order – for example, an event involving two particle-photon interactions is determined from the second term (since H_{int} appears twice here). Moreover,

Ann. Phys. (Berlin) **526**, No. 3–4 (2014)

annalen
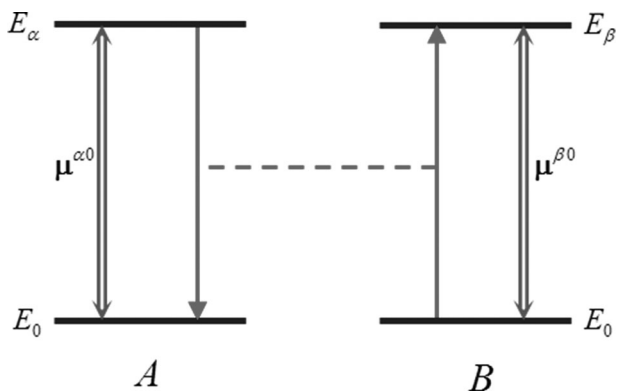der **physik**

Review Article

Figure 2 Energetic scheme for resonance energy transfer, $A^\alpha + B^0 \rightarrow A^0 + B^\beta$. Dark blue horizontal lines denote states of donor A or acceptor B; red vertical arrows represent electronic transitions between such states. The dashed red lines show virtual photon coupling between the nanoparticles, and the blue vertical double-headed arrows denote transition dipole moments corresponding to the adjacent electronic transition.

$T_0 \approx (E_I - H_0)^{-1}$ denotes an energy denominator in which $H_0 = H_{\text{part}} + H_{\text{rad}}$ is the unperturbed Hamiltonian that operates on virtual intermediate states, and E_I is the energy of state $|I\rangle$.

In the simplest form, the coupling of electrically neutral particles involves the interaction of their electric dipoles (whether static or dynamic) through virtual photon mediation, as represented by Fig. 1(b). On the transfer of electronic excitation this coupling is known as resonance energy transfer (RET) as depicted by Fig. 2; an in-depth investigation on RET processes is given in Sec. 5. In terms of QED, dipole coupling is interpreted as involving the creation of a virtual photon at a particle A and its subsequent annihilation at B. However, since all conceivable time-orderings must be included, the converse sequence must also be accommodated. The latter is required since the initial and final (energy-conserved) system states are observable, but the exact configuration of the intermediate state is non-detectable: as a result, all possibilities – two in the above example – must be deployed in such a QED calculation. Virtual photons play a part in these intermediate states, and they too are said to be non-detectable. In terms of the time-energy uncertainty principle, which allows for the non-conserving intermediate states, the 'existence' of a virtual photon is due to the 'borrowing' of energy from the background energy of the vacuum; although a virtual photon must 'repay' this energy after a very-short period.

In general terms, the quantum amplitude for the pairwise coupling between electric dipoles (μ^A and μ^B) is

expressed as [12]:

$$M_{FI} = \mu_i^A V_{ij}(k, \mathbf{R}) \mu_j^B, \tag{4}$$

where implied summation over Cartesian indices i and j is used, $\hbar c k$ denotes the energy (if any) transferred from A to B; $\mathbf{R} = \hat{\mathbf{R}} R$ is the displacement between A and B, and the electromagnetic coupling tensor, $V_{ij}(k, \mathbf{R})$, is given by:

$$V_{ij}(k, \mathbf{R}) = \frac{e^{ikR}}{4\pi\varepsilon_0 R^3} \left\{ \left(\delta_{ij} - 3\hat{R}_i\hat{R}_j\right) - \left(ikR\right) \right.$$
$$\left. \times \left(\delta_{ij} - 3\hat{R}_i\hat{R}_j\right) - (kR)^2 \left(\delta_{ij} - \hat{R}_i\hat{R}_j\right) \right\}. \tag{5}$$

From this expression, which encapsulates the behaviour of the virtual photon, it is ascertained that the first term dominates in the short-range or near-field region ($kR \ll 1$), and the last term in the long-range or wave-zone ($kR \gg 1$). Individually, the initial and final terms of Eq. (5) effectively signify an electromagnetic mediator of completely 'virtual' and 'real' characteristics, respectively [13]. However, for dynamic coupling ($k \neq 0$), which corresponds to energy transfer, neither term may be considered in isolation. As the dynamic interaction occurs over an increasing distance, the associated energy transfer exhibits an increasingly 'radiative', propagating behaviour – although a partial virtual character always remains. Equally, at small distances, the form of energy transfer normally termed 'radiationless' retains some attributes of 'real' photon exchange. In contrast, permanent dipole interactions or static coupling ($k = 0$), corresponding to the first term of Eq. (5) alone, relate to purely virtual photon exchange.

Returning to the dynamic case, the effective character of the virtual photon in the near-field fundamentally differs to the wave-zone. One of the most significant aspects of this dissimilarity can be understood from a perspective based on Helmholtz's theorem. This states that any vector field, Ξ, can be decomposed into curl-free (longitudinal or irrotational, *irr*) and divergence-free (transverse or solenoidal, *sol*) components namely $\Xi = \Xi^{irr} + \Xi^{sol}$, in which $\nabla \times \Xi^{irr} = 0$ and $\nabla \cdot \Xi^{sol} = 0$. In non-relativistic QED where the Coulomb gauge is usually deployed, the vector potential has no divergence, and the solenoidal component alone need be considered. The transversality of the vector potential means that, for each electromagnetic mode, the propagating electric and magnetic vector fields are disposed orthogonally to the propagation vector $\mathbf{k}$. However, the character of the virtual photon is less straightforward since different features emerge in near- and far-field couplings. Close to

their emitter, photons are subject to a significant degree of quantum uncertainty in vector momentum, including their direction of propagation. In consequence, on summing over all virtual photon modes (as outlined previously), the near-field reveals not only components that are transverse, but also some components that are longitudinal with respect to the displacement vector **R**. However, over longer distances, the longitudinal components decay until the behaviour is almost consistent with a fully transverse field. This far-field region, connected to remote detection, is accordingly associated with 'real' photon exchange. For more on the latest theories concerning the concept of virtual photons see references [14, 15]. The rest of this review departs from these fundamental issues; we now explore the variety of nanoscale processes mediated by virtual photons.

3 Virtual photons in nanomechanical coupling

Casimir-Polder effect. Many fundamental optical properties deriving from nanoparticle couplings rely on virtual photons to act as the mediator. A well-known example is the Casimir effect that typically operates over nanoscale dimensions between electrically conductive surfaces; the classic model involves two uncharged metallic plates in a vacuum [16, 17]. However, similar principles apply to a much broader range of systems, with equally important consequences for any closely positioned, neutral and non-polar nanoparticles. This Casimir-Polder effect in turn relates to the van der Waals or dispersion interaction [18–24], which was first characterized in London's calculation of an R^{-6} dependence for such couplings. The latter distance-dependence proves perfectly valid in the short-range region, analogous to the interacting permanent dipoles case of Sec. 2. However, by employing a quantum electrodynamical formulation, the interaction can be understood as involving the creation of short-lived virtual photons from the vacuum, and on this basis Casimir and Polder determined not only the short-range limit, but also a change to an asymptotic R^{-7} dependence over longer distances [25]. This effect is consistent with the acquisition of 'real' photon attributes, and retardation effects relating to the finite speed of light, that do not apply in the permanent dipole case. In the following, to circumvent much mathematical complexity, we focus on particles in close proximity within the non-retarded limit.

In terms of quantum electrodynamics, the dispersion interaction entails two dipole-dipole couplings, mediated by two virtual photons, and corresponds to the four particle-photon couplings shown in Fig. 1(c) and, thus,

the fourth term of Eq. (3). Although for the present static (short-range) coupling case, where retardation effects in the virtual photon exchange are negligible, it is more convenient to determine an expression for the dispersion interaction from the second term of Eq. (3), with H_{int} then relating to the first term of Eq. (5). A further caveat is that, since an optical property (such as the dispersion interaction) involves identical initial and final states, the measurable quantity is defined as a potential energy ΔE, rather than a quantum amplitude [26]. The resulting expression involves a summation over the intermediate (virtual) states s and t, and is ascertained as [27]:

$$\Delta E = -\sum_{s,t} \frac{\mu_i^A V_{ij}(0, \mathbf{R}) \mu_j^B \mu_m^A V_{mn}(0, \mathbf{R}) \mu_n^B}{E_{s0}^A + E_{t0}^B}, \tag{6}$$

where the denominator, within which $E_{s0} = E_s - E_0$ is the energy difference between the intermediate and ground state, derives from T_0 in Eq. (3) and $V_{ij}(0, \mathbf{R})$ is the static electromagnetic coupling tensor corresponding to the first term of Eq. (5). The numerator is essentially a square of the right-hand side of Eq. (4), signifying that two simultaneous dipole-dipole interactions arise in the dispersion interaction. The mechanical force acting between A and B is apparent following determination of the dispersion force via the expression $\mathrm{F} = -\partial(\Delta E)/\partial \mathbf{R}$; an R^{-7} dependence is discovered in the short range. Since electromechanical devices are becoming increasingly available at the nanoscale – underpinning the technology now known as NEMS [28–32] – the role of the Casimir effect cannot be ignored in a treatment of its mechanical properties (Fig. 3). In fact it is now recognized that the Casimir effect is the primary cause of stiction or pull-in instabilities, *i.e.* the moving parts of the device become to some extent adhesive to the fixed electrode, leading to lose of functionality [33–43]. Alternatively, exploiting the effect, nanoelectromechanical switches requiring the Casimir force to act as the actuator have been proposed [44, 45].

Burgeoning interest in the Casimir effect has arisen in recent years, leading to further advancement in the theoretical and experimental studies on the subject. An intriguing discovery is that the Casimir force may become repulsive [46–49], usually by immersing suitably interacting materials into a dielectric fluid with specified dielectric properties, leading to the possibility that repulsion of this type may enable quantum levitation [50–54]. Additionally, there is much activity relating to the phenomenon of 'quantum friction' [55–59], *i.e.* the friction experienced by a pair of dielectric particles in relative motion even at absolute zero (at such a temperature any fluctuations must be solely quantum in nature).
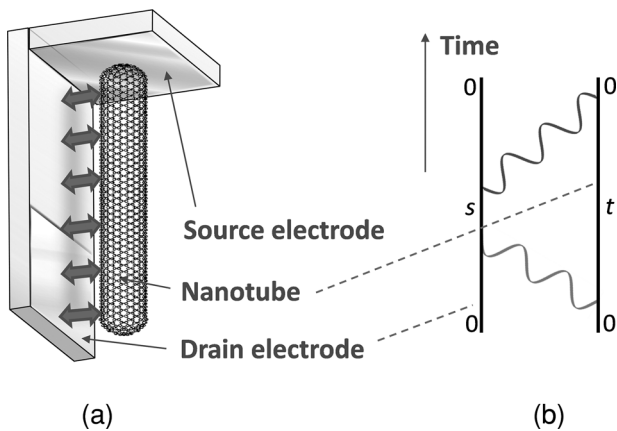
Ann. Phys. (Berlin) **526**, No. 3–4 (2014)

annalen der **physik**

Review Article

Figure 3 NEMS switching device based on electrically induced deformation of a carbon nanotube. (a) Schematic structure: red arrows denote mechanical forces on the nanotube due to an applied voltage. The influence of an attractive Casimir force must also be considered, since the effect may cause device failure as a result of stiction; (b) One of the Feynman diagrams for calculating the Casimir force, 0 denoting a ground state configuration and s and t as intermediate (virtual) states, with virtual photons propagating between the nanotube and drain electrode plate.

Similarly, it has been observed that a dynamical Casimir effect, in which a driven mechanical motion produces an oscillatory field, permits the conversion of vacuum fluctuations into 'real' photons [60]. Theoretical procedures can now accurately predict non-additive van der Waals potentials in many-body problems [61–63], which cannot be effectively modelled using a pairwise summation approach. Moreover, calculations of the Casimir force in various structural configurations, including periodically deformed objects, have also advanced [64–70]. It is now anticipated that these results may lead to the tailoring of Casimir physics through specific geometric designs.

Optical binding. Now consider a very different category of material system – one that comprises micro- or nano-particles held in suspension (usually by the use of optical tweezers instrumentation [71–74]). When two or more such particles are trapped in close proximity, the effect on the interacting pair of a throughput laser beam can lead to the phenomenon of optical binding [75–84], generating forces that may override the intrinsic dispersion interaction. A recurrent motif in experiments of this type is the application of counter-propagating laser beams (for example, see ref. [85]), which ensures radiation pressure due to the beam cancels out; optical binding then becomes the most significant force over nanoscale distances. At present this phenomenon is incompletely understood, and several mechanisms may come into play according to the sizes

of the particles involved [81]. For this reason it is important that experimental and theoretical research remains concurrent – to enable comprehension of the underlying mechanism, accompanied by new techniques for optical manipulation.

Although a variety of optical processes are effective for particles with dimensions approaching or exceeding the wavelength of the throughput beam, the case of non-contact interactions between 'Rayleigh particles' has a specifically quantum electrodynamical origin. In detail, the mechanism entails an elastic forward-scattering of a passive (off-resonant laser) beam, without any net absorption or stimulated emission, mediated by virtual photon exchange between the particles (Fig. 4). This phenomenon, first predicted using the virtual photon formalism [86], has increasingly been advocated as a tool for the optical manipulation and configuration of particles, and many optically induced arrays have been observed experimentally [75, 85, 87].

In terms of QED, the optical binding potential between two interacting nanoparticles, over all displacements **R**, emerges as:

$$\Delta E = \left(\frac{I}{2\,\varepsilon_0 c} \right) e_i \bar{e}_n \, \mathrm{Re} \left(\alpha_{ij}^A \, V_{jm}(k, \mathbf{R}) \, \alpha_{mn}^B \mathrm{e}^{-ik \cdot \mathbf{R}} \right.$$
$$\left. + \; \alpha_{ij}^B \, V_{jm}(k, \mathbf{R}) \, \alpha_{mn}^A \mathrm{e}^{ik \cdot \mathbf{R}} \right), \tag{7}$$

where the argument, k, of the coupling tensor equates to the wave-number of the laser radiation. In each term on the right of Eq. (7) are four factors of significance. These are: (*i*) optical response tensors associated with the relevant nanoparticles, in this case the polarisability tensor α_{ij}, denoting simultaneous photon emission and absorption; (*ii*) the coupling tensor $V_{jm}(k, \mathbf{R})$, which (as stated earlier) describes the form of electromagnetic interaction between the nanoparticles; (*iii*) the optical polarization vector **e** and intensity I, which are properties of the irradiating laser; (*iv*) the phase factors $\mathrm{e}^{\pm ik \cdot \mathbf{R}}$, reflecting the absorption and emission of laser photons at two different positions. Moreover, the first term of Eq. (7) corresponds to the laser beam entering at A and exiting at B; the second term the converse. The optical binding force is found by inserting Eq. (7) into the earlier force expression; this results in the discovery of an R^{-4} distance dependence for the short-range region.

It is noteworthy that a photon from the input beam is treated as wholly 'real', in that the photon has a single precise wave-vector and polarisation (rather than a sum over all possibilities), which is consistent with the light source being in the long-range region compared to the particle pair. In principle this ought to be construed as an approximation (although a very good one) since, as
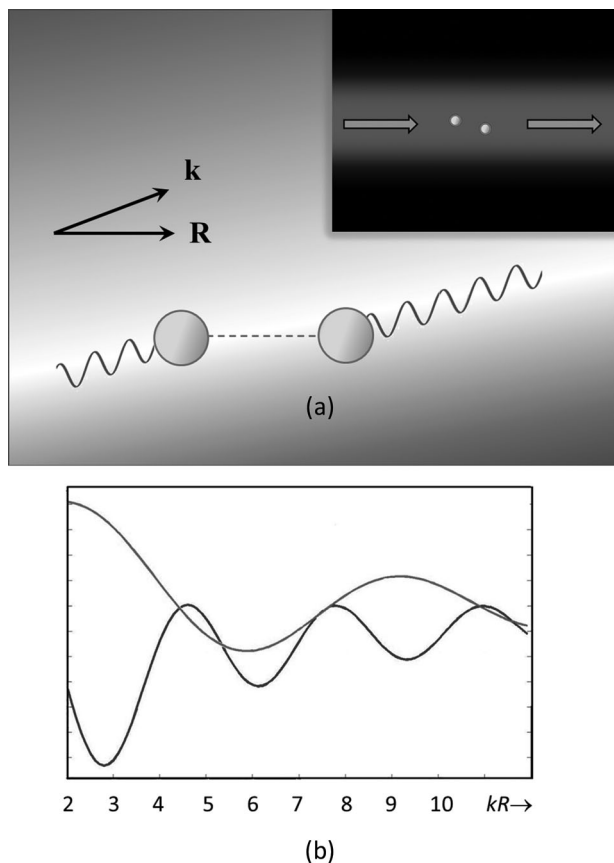
Figure 4 (a) Graphical representation of optical binding. Laser light (wave-vector **k**, field depicted by blue wavy lines) arrives at *A* on the left and, displaced along a vector **R**, departs from *B* on the right; the nanoparticle pair *A-B* are coupled together by a virtual photon (red dashed line). Inset represents the pair positioning and orientation within the encompassing laser beam. (b) Variation of the optically induced potential as a function of *kR* (arbitrary vertical scale). Blue line – particles along the beam axis, **k** ∥ **R**; red line – pair oriented across the beam, **k** ⊥ **R**. In the former, more common case, the potential minimum at $kR \sim 3$ (typically signifying distances below ~ 200 nm) gives the strongest optical binding effect.

explained in Sec. 2, photons will always retain some virtual characteristics.

4 Nonlinear optical applications

In the field of nonlinear optics, light frequency-conversion falls into two main classes. Most common are *parametric* processes, where no net transfer of energy or momentum from the electromagnetic field to the material occurs, and conversion is essentially instantaneous: second harmonic generation is a familiar

example. In contrast, *non*-parametric nonlinearities involve the resonant excitation of nanoparticles within the irradiated material, usually with energy transfer to other electronic levels before emission. Such processes are usually less energy-efficient, but may be effective at significantly lower levels of input intensity. In experimental reports [88–96], rare-earth doped crystals or glasses are the most commonly used materials in such processes. The crucial energy transfer stages generally operate through dipole-dipole coupling between ions, again meditated by virtual photon exchange. Processes involve differing initial and final states and, therefore, relate to the quantum amplitude M_{FI} rather than energy potentials [26]; the modulus square of M_{FI} corresponds to the experimentally measureable rate (*vide infra*). We shall focus on results for non-parametric nonlinearities known as frequency upconversion, sensitisation and quantum cutting, all of which are processes that engage three interacting ions. As detailed below, upconversion – in which low frequency photoexcitation is converted to a higher frequency – shares common theoretical ground with sensitisation, where a dopant assists the conveyance of excitation between donor and acceptor, and quantum cutting (the time-inverse of upconversion).

The pooling of excitation energy from two donor ions (*A* and *B*) to an acceptor ion *C*, a process commonly categorised as upconversion, is represented by:

$$A^\alpha + B^\beta + C^0 \longrightarrow A^0 + B^0 + C^\gamma. \tag{8}$$
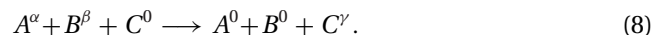
Here, the Greek superscripts indicate a nanoparticle in an excited state, while 0 denotes the ground electronic state, and the excitation energy transferred to *C* is approximately the sum of the energies on *A* and *B*. As shown by the energetics scheme of Fig. 5, the pooling process has two guises: one is the transfer of excitation from *A* and *B* directly to *C*, known as *cooperative* transfer; the other entails excitation transferal from *A* to *B* (or *vice-versa*) and combined energy transfer to *C*, named *accretive* transfer. The quantum amplitude for the excitation pooling process is given by:

$$M_{FI} = \mu_i^A V_{ij}\left(k, \mathbf{R}''\right) \alpha_{jm}^C V_{mn}\left(k, \mathbf{R}'\right) \mu_n^B$$
$$+ \mu_i^A V_{ij}\left(k, \mathbf{R}\right) \alpha_{jm}^B V_{mn}\left(k, \mathbf{R}'\right) \mu_n^C$$
$$+ \mu_i^B V_{ij}\left(k, \mathbf{R}\right) \alpha_{jm}^A V_{mn}\left(k, \mathbf{R}''\right) \mu_n^C, \tag{9}$$

where $\mathbf{R}' = \mathbf{R}_C - \mathbf{R}_B$ and $\mathbf{R}'' = \mathbf{R}_C - \mathbf{R}_A$; the first term corresponds to cooperative transfer, and the other two terms to accretive transfer. Since the observable emission intensity relates to M_{FI} squared, the resulting cross-terms physically denote quantum interference between

Ann. Phys. (Berlin) **526**, No. 3–4 (2014)
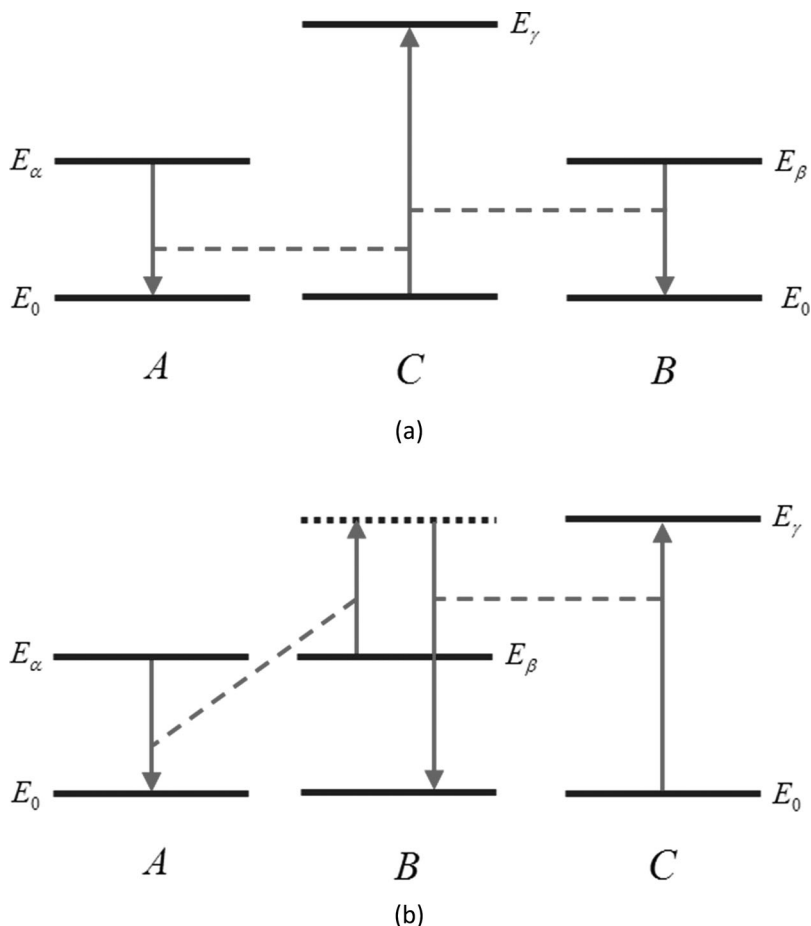
annalen
der **physik**

Review Article

Figure 5 Energetic schemes for energy pooling mechanisms: (a) cooperative transfer; (b) accretive transfer. Blue dashed line denotes a virtual state.

the sub-mechanisms – for example between cooperative and accretive transfer.

Rare earth sensitisation is implicated in a variety of photophysical processes – the nature of which is, in all cases, defined by the involvement of a bridge nanoparticle (the sensitiser) in assisting excitation transfer. The specific case investigated here is where the acceptor *C*, initially in a pre-excited state *β*, absorbs excitation from a donor *A* in the presence of a sensitiser *B*. This is represented by:

$$A^{\alpha}+C^{\beta} \xrightarrow{B^{0}} A^{0} + C^{\gamma}, \tag{10}$$

and the corresponding scheme is given by Fig. 6. The quantum amplitude for the sensitisation process has a similar form to Eq. (9), the main difference being that the sensitiser relates to a permanent dipole, rather than a transition dipole, since *B* begins and ends at the ground state. On the assumption that the lanthanide ions are in a centrosymmetric environment, *B* cannot have a permanent dipole and, therefore, the first and third terms of Eq. (9) – more precisely, the analogous expression for sensitisation – must give null results; in contrast, *B* is

assigned to a static polarisability tensor in the second term. As a consequence, it is deduced that the sensitisation process is purely accretive and quantum interference does not occur [97]. The process of quantum cutting (or down-conversion) is identical to up-conversion except that the energy flows from *C* to *A* and *B* – *i.e.* higher frequency excitation is converted into lower frequencies – as shown by Fig. 7. Quantum cutting is represented by Eq. (8) but time-reversed (that is, traversing from right to left) and its quantum amplitude is again of similar form to Eq. (9).

5 Resonance energy transfer processes

Resonance energy transfer is the primary mechanism by means of which electronic energy migrates between amenable nanoparticles [98–102]. Current research on energy transfer is diverse and spans the natural sciences. The assortment of applications is evident from two representative examples: at one end of the spectrum, RET features in bioanalysis techniques where luminescence from a quantum dot bioprobe is quenched in response to
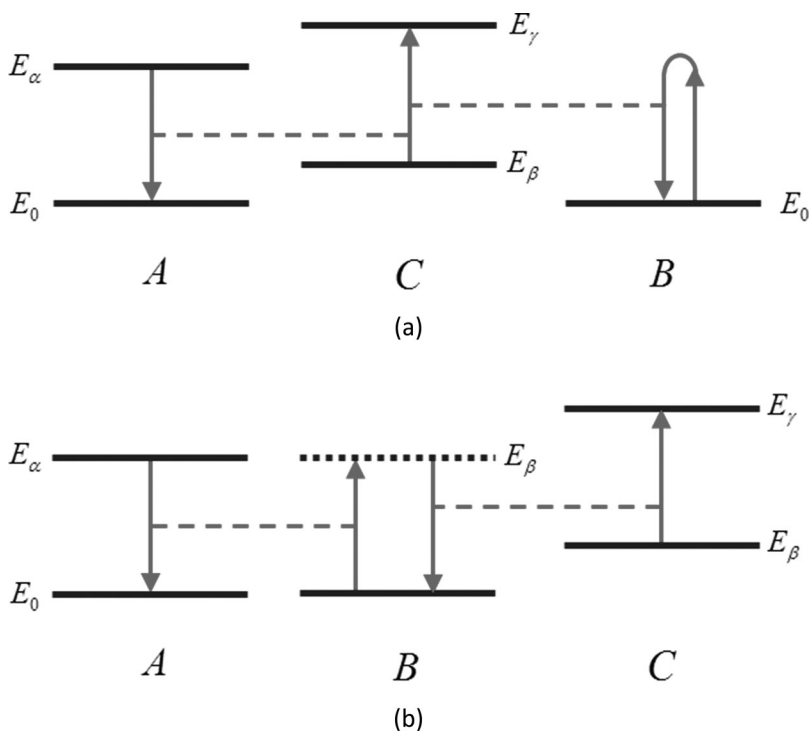
Figure 6 Energetic schemes for sensitisation mechanisms: (a) cooperative transfer; (b) accretive transfer.

chemical binding to biological targets [103–107] (which arises since an alternative relaxation pathway is provided by RET); the other extreme is exemplified by the enhancement of quantum entanglement between two distant qubits, due to strengthened dipole-dipole coupling through use of a plasmonic nano-waveguide [108–111].

In this section, a discussion is given on energy transfer within nanostructures containing a multitude of sub-units – specific examples, ranging from polymers to photosynthetic systems, are found in refs [106, 112–118]. But initially let us re-examine the elementary act of energy migration from donor A to acceptor B, where the electronic energy lost and gained in the two sub-units (henceforth termed chromophores) must be equal for energy to be conserved; although, within the ultrafast timescale for the energy migration, a temporary relaxation of exact conservation in isolated photon creation and annihilation events may arise.

In cases where the donor decay largely occurs through energy transfer rather than direct fluorescence, the transfer efficiency of RET from A to B, primarily quantified by a rate denoted by Γ, is taken from the Fermi-Golden rule and written as [119]:

$$\Gamma = \frac{2\pi}{\hbar} |M_{FI}|^2 \delta \left(E_{\alpha 0} - E_{\beta 0} \right), \tag{11}$$

where the quantum amplitude, M_{FI}, is expressed by (4), and $E_{\alpha 0} = E_\alpha - E_0$ and $E_{\beta 0} = E_\beta - E_0$ are the ener-

gies associated with the electronic transitions $|\alpha\rangle \to |0\rangle$ and $|0\rangle \to |\beta\rangle$, respectively; the Dirac delta $\delta(E_{\alpha 0} - E_{\beta 0})$ serves to enforce the energy conservation. In fact, since each electronic state has its own manifold of vibrational energy levels, the transfer depends on a superposition of the continuous spectra associated with both electronic transitions $|\alpha\rangle \to |0\rangle$ and $|0\rangle \to |\beta\rangle$. While the result delivered by Eq. (11) also includes (within its quantum amplitude quadratic term) geometric factors relating to the orientational disposition of the transition moments, isolation of the more significant distance-dependence is given by performing a rotational average. Accordingly, the rate expression becomes:

$$\Gamma = \frac{2\pi}{9\hbar} \left|\mu^A\right|^2 \left|\mu^B\right|^2 A(k, R) \delta \left(E_{\alpha 0} - E_{\beta 0} \right), \tag{12}$$

where the dependence of RET on the distance R is thus embedded within a function $A(k, R)$, defined by [12, 13]:

$$A(k, R) = V_{ij}(k, \mathbf{R}) \bar{V}_{ij}(k, \mathbf{R})$$
$$= \left(8\pi^2 \varepsilon_0^2 R^6\right)^{-1} \left[3 + k^2 R^2 + k^4 R^4\right]. \tag{13}$$

Two familiar forms of photophysical behaviour are encompassed by Eq. (13), as illustrated in Fig. 8. In the short-range region, the first term dominates and gives the overall R^{-6} dependence of the Förster theory of radiationless transfer; physically, this term is associated with a photon mediator of completely virtual nature.
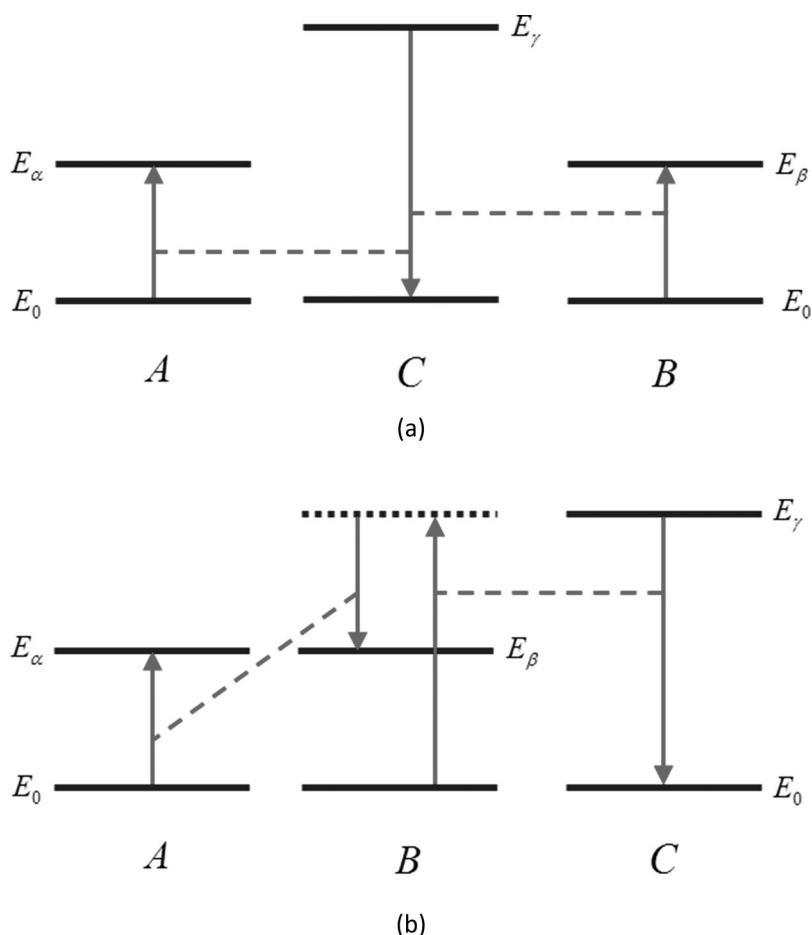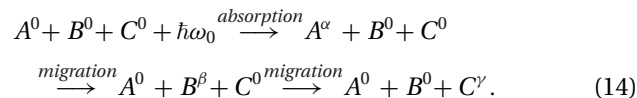
Ann. Phys. (Berlin) **526**, No. 3–4 (2014)

annalen
der **physik**

Figure 7 Energetic schemes for quantum cutting (down-conversion) mechanisms: (a) cooperative transfer; (b) accretive transfer.

In contrast, in the long-range, the final term of Eq. (13) dominates – this contains an inverse square dependence on distance that characterises radiative transfer involving 'real' photon exchange. Furthermore, there is an intermediate set of separations where the middle term, in R^{-4}, also plays a significant role. The comprehensive result (13) unifies these, apparently disparate, forms of photophysical behaviour, and clarifies their common physical origination.

In principle the simplest mechanism for energy migration is one in which, after photon absorption, the excitation transfers directly to its destination – visiting no intermediary chromophores en-route. However, in nanostructured materials whose architectures contain a large number of sub-units, the physical sites of initial excitation (usually where there is photon absorption), and a central energy trap, may be quite remote in nanoscale terms, and accordingly this direct migrational route is highly unlikely. This is because intermediary chromophores enable an alternative route – a sequence of short steps from the initial excitation site to the destination. The latter is a much more efficient route,

compared to a single 'hop', due to the sharply diminishing distance dependence (*i.e.* R^{-6}). To proceed, A and B are designated as chromophores that, under certain conditions, may act as donors or acceptors on each transfer step, and C is introduced as the destination unit. There are a variety of electrodynamical mechanisms by means of which light is absorbed and transported to the destination unit [120–123]. The simplest example is written as:

$$A^0 + B^0 + C^0 + \hbar\omega_0 \stackrel{absorption}{\longrightarrow} A^\alpha + B^0 + C^0$$
$$\stackrel{migration}{\longrightarrow} A^0 + B^\beta + C^0 \stackrel{migration}{\longrightarrow} A^0 + B^0 + C^\gamma. \quad (14)$$

Here, the incident photon $\hbar\omega_0$ is absorbed (annihilated) at A, and the resulting excitation is transferred to the destination C via two transfer 'hops'; this is illustrated by Fig. 9. The latter involves B acting as both acceptor and donor during the migration. In the transport of electronic excitation between chromophores, which is mediated by virtual photon exchange, the pairwise energy transfer (dynamic) process of Sec. 2 is the most probable to occur. However other, higher order mechanisms
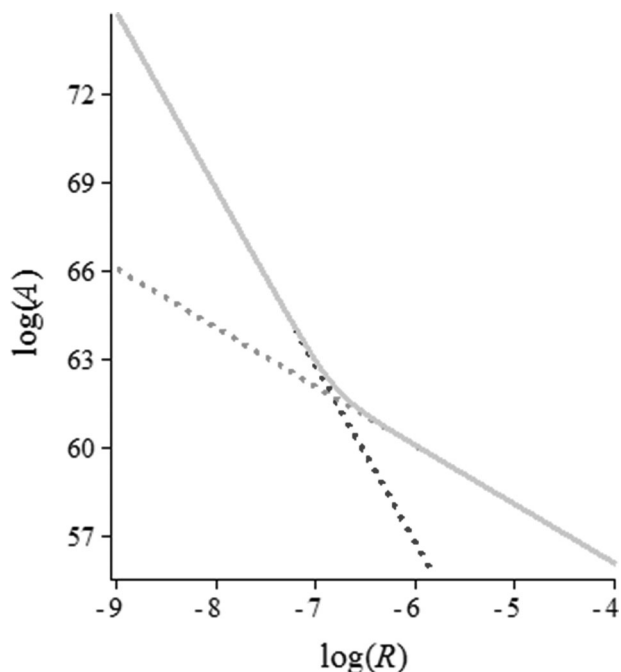
Figure 8 Log-log plot of the *A* function (quantifying the energy transfer rate) against the interparticle displacement *R* (in metres). Yellow line represents the *A* function in arbitrary units; green and blue dotted lines indicate an R^{-2} and R^{-6} dependences, respectively. The behaviour is consistent with reasoning that virtual photon behaviour occurs in the near-field, over which R^{-6} dominates, and increasingly 'real' characteristics are observed in the wave-zone where R^{-2} prevails.

may arise, such as two-photon resonance energy transfer – where a chromophore absorbs two photons and transfers the combined energies to another – and the pooling processes of Sec. 5 as shown in Fig. 10. Perhaps surprising is the fact that virtual photon exchange may also be involved in the initial absorption step, as will now be shown.

First consider a single-photon absorption mechanism that involves excitation of two chromophores. This process is known as *cooperative single-photon* absorption, and is represented by:

$$A^0 + B^0 + \hbar\omega_0 \longrightarrow A^\alpha + B^\beta. \tag{15}$$

the energetics of which is illustrated in Fig. 11(a). This type of mechanism is higher order compared to conventional single-photon absorption. As a consequence, cooperative absorption can be anticipated under conditions where incident photons are not resonant to an electronic transition within a chromophore – since conventional absorption is excluded in such a case. The

quantum amplitude of the process is given as follows:

$$M_{FI} = e_i \alpha_{ij}^A V_{jm} \mu_m^B + \mu_i^A V_{ij} \alpha_{jm}^B e_m, \tag{16}$$

where the first term corresponds to an electrodynamic mechanism in which an absorption at *A* is associated with an energetic redistribution to *B*; the latter, via virtual photon exchange. In contrast, the second term involves initial photon absorption at *B*, which is reflected in the reversal of the optical response tensors corresponding to *A* and *B*.

A second process is termed *mean-frequency absorption*, which involves excitation of two chromophores by the simultaneous absorption of two photons. This type of absorption is represented by:

$$A^0 + B^0 + \hbar\omega_0 + \hbar\omega_0' \longrightarrow A^\alpha + B^\beta, \tag{17}$$

with energetics as shown in Fig. 11(b). This process is observable when the two incident photons are off-resonant with respect to electronic transitions within both chromophores, and its quantum amplitude is written as:

$$M_{FI} = e_i' \alpha_{ij}^A V_{jm} \alpha_{mn}^B e_n + e_i \alpha_{ij}^A V_{jm} \alpha_{mn}^B e_n'. \tag{18}$$

Here, off-resonant single-photon absorption occurs at each chromophore, accompanied by energy redistribution via virtual photon mediation – the prime indicates which chromophore initially absorbs $\hbar\omega_0'$. It is worth emphasizing that such processes – which may also be observed in the gas phase as a result of collisional energy redistribution – can nonetheless occur simply through nanoscale proximity between the participating chromophores; it need not require the involvement of motion or collisional perturbations.

6 Conclusions and future directions

Although remaining relatively unknown, photons commonly characterised as either 'real' or 'virtual' are in fact two extremes of a continuum of behaviour. However, even if the distinction were to be regarded as illusory (or even to an extent, largely semantic) it remains the case that the attributes identified with virtual photon exchange are present in nanoscale interactions. The principal examples offered in this review include widely disparate topics, such as inter-particle transfer of electronic excitation, the laser-induced forces between particles known as optical binding, non-parametric frequency-conversion processes, the intricate mechanisms of light-harvesting materials including dendrimeric polymers and quantum dot-based systems, and nanomechanical
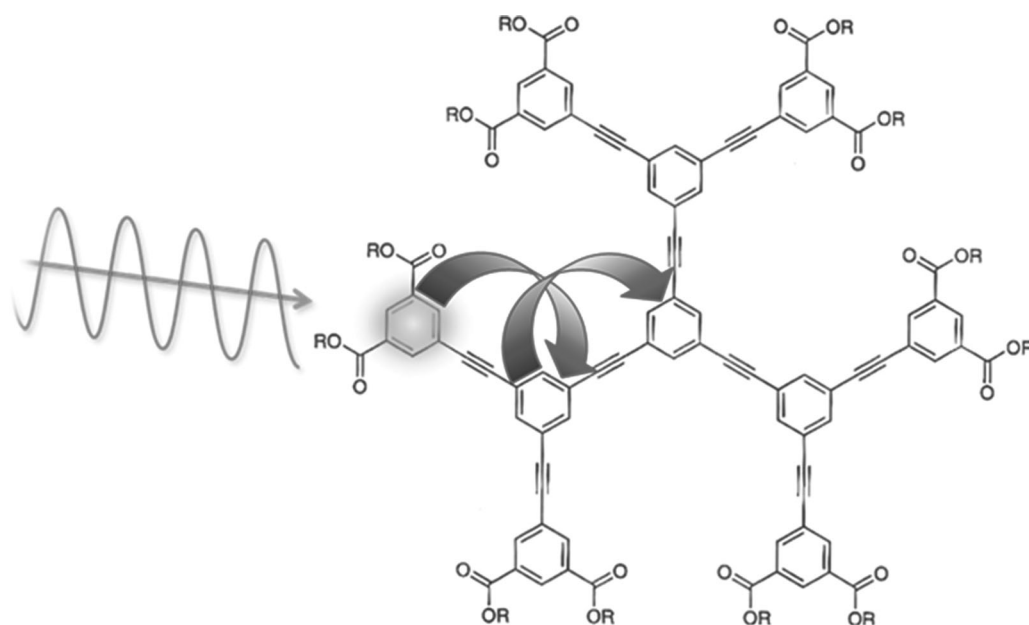
Ann. Phys. (Berlin) **526**, No. 3–4 (2014)

annalen
der **physik**

Figure 9 Two-step light harvesting mechanism illustrated schematically in a second-generation dendrimer. A peripheral group, initially excited by 'real' photon absorption, then acts as a donor for energy transfer to a neighbouring first-generation acceptor; this then acts as a donor for energy transfer to the core unit.
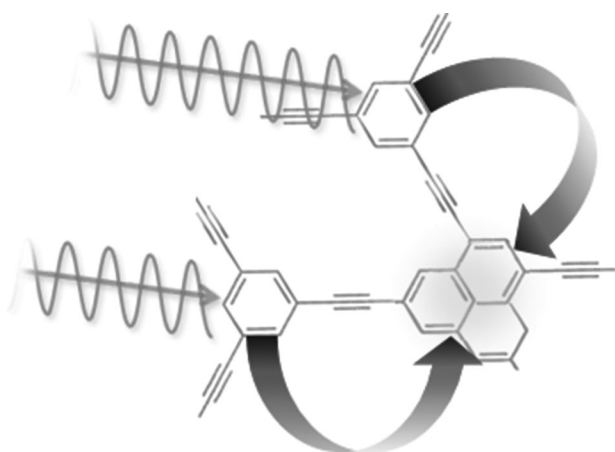

Figure 10 Light harvesting mechanism for delivering the energy of two photons, captured by two peripheral groups, to a chemically linked common neighbour (specific dendrimer components shown only for illustration). The pooling mechanism, which follows the initial excitation, is identical to Fig. 5(a).

systems based on the Casimir effect. A sample of the latest research, based on dipole-dipole coupling mediated by virtual photon exchange, has also been included.

Looking to the future, the direction of further progress is expected to be influenced by two main factors. One is the exploitation of recent advances in calculational methods, which now offer opportunities to perform calculations on the electromagnetic coupling between a
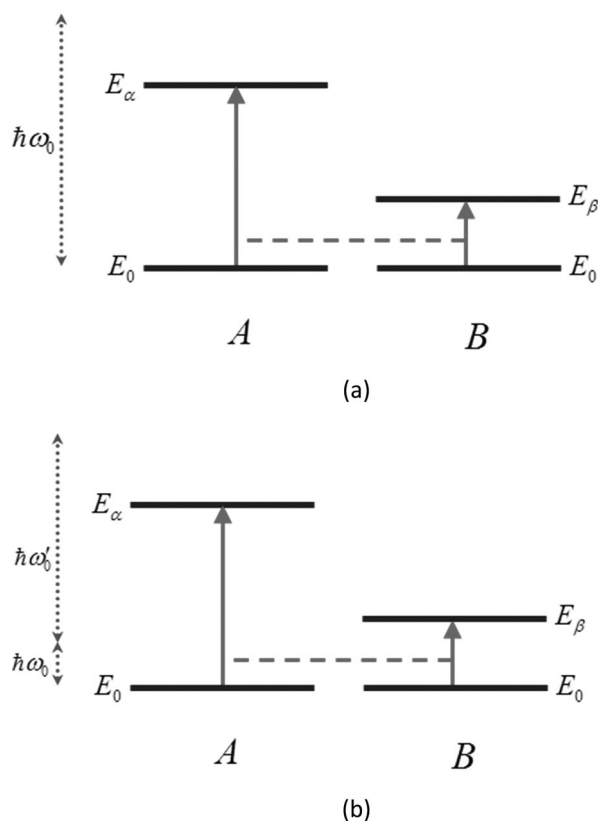

Figure 11 Energetic scheme for: (a) cooperative single-photon absorption and (b) mean-frequency absorption. The red double-head arrows represent the energy of the incoming photon(s).

Review Article

large number of particles. The other is the facility presented by modern molecular modelling and simulation software, enabling pursuit in detailed quantitative measure of the electrodynamic mechanisms operating in actual materials. As these advances facilitate extensions of the kind of analysis presented in this review, a strong case is made that virtual photons are becoming increasingly prominent at the very heart of modern nanophotonics.

Key words. Casimir force, NEMS (nanoelectromechanical systems), QED (quantum electrodynamics), optical binding, NLO (nonlinear optics), up-conversion, RET (resonance energy transfer), energy harvesting.

David L. Andrews is a Professor and leads the nanophotonics and quantum electrodynamics research group at the University of East Anglia, Norwich, UK. His research interests are currently centring on resonance energy transfer, optomechanical forces, optical vortices, and nonlinear optics.

David S. Bradshaw received his Ph.D. degree in physics from the University of East Anglia (UEA), Norwich, UK, in 2006. He is now a postdoctoral researcher at UEA with research focuses on resonance energy transfer and optomechanical forces.

References

[1] P. W. Milonni, The Quantum Vacuum: An Introduction to Quantum Electrodynamics (Academic Press, San Diego, 1993).

[2] F. Halzen and A. D. Martin, Quarks and Leptons: An Introductory Course in Modern Particle Physics (Wiley, New York, 1984).

[3] C. Cohen-Tannoudji, J. Dupont-Roc, and G. Grynberg, Photons and Atoms: Introduction to Quantum Electrodynamics (Wiley, New York, 1989).

[4] C. Cohen-Tannoudji, J. Dupont-Roc, and G. Grynberg, Atom-Photon Interactions: Basic Processes and Applications (Wiley, New York, 1998).

[5] D. P. Craig and T. Thirunamachandran, Molecular Quantum Electrodynamics: An Introduction

to Radiation-Molecule Interactions (Dover Publications, Mineola, NY, 1998).

[6] R. G. Woolley, Proc. R. Soc. A **456**, 1803–1819 (2000).

[7] I. Lindgren, S. Salomonson, and D. Hedendahl, Int. J. Quant. Chem. **108**, 2272–2279 (2008).

[8] A. Salam, Molecular Quantum Electrodynamics: Long-Range Intermolecular Interactions (Wiley, Hoboken, NJ, 2009).

[9] J. D. Jackson, Classical Electrodynamics (Wiley, New York, 1998).

[10] A. Zangwill, Modern Electrodynamics (Cambridge University Press, Cambridge, 2012).

[11] C. H. Wilcox, Perturbation Theory and its Applications in Quantum Mechanics (Wiley Chapman and Hall, New York, London, 1966).

[12] G. J. Daniels, R. D. Jenkins, D. S. Bradshaw, and D. L. Andrews, J. Chem. Phys. **119**, 2264–2274 (2003).

[13] D. L. Andrews and D. S. Bradshaw, Eur. J. Phys. **25**, 845–858 (2004).

[14] C. Roychoudhuri, A. F. Kracklauer, and K. Creath, The Nature of Light: What is a Photon? (CRC Press, Boca Raton, 2008).

[15] D. L. Andrews, J. Phys. Chem. Lett. **4**, 3878–3884 (2013).

[16] H. B. G. Casimir, Proc. K. Ned. Akad. Wet. **60**, 793–795 (1948).

[17] R. L. Jaffe and A. Scardicchio, Phys. Rev. Lett. **92**, 070402 (2004).

[18] A. E. Cohen and S. Mukamel, Phys. Rev. Lett. **91**, 233202 (2003).

[19] S. K. Lamoreaux, Rep. Prog. Phys. **68**, 201–236 (2005).

[20] J. M. Obrecht, R. J. Wild, M. Antezza, L. P. Pitaevskii, S. Stringari, and E. A. Cornell, Phys. Rev. Lett. **98**, 233202 (2007).

[21] S. Y. Buhmann and S. Scheel, Phys. Rev. Lett. **100**, 253201 (2008).

[22] Y. Sherkunov, Phys. Rev. A **79**, 244107 (2009).

[23] J. Rodríguez and A. Salam, Phys. Rev. A **82**, 062522 (2010).

[24] J. Rodríguez and A. Salam, J. Chem. Phys. **133**, 164501 (2010).

[25] H. B. G. Casimir and D. Polder, Phys. Rev. A **73**, 360–372 (1948).

[26] D. S. Bradshaw and D. L. Andrews, J. Phys. Chem. A **117**, 75–82 (2013).

[27] D. L. Andrews, D. S. Bradshaw, J. M. Leeder, and J. Rodríguez, Phys. Chem. Chem. Phys. **10**, 5250–5255 (2008).

[28] H. G. Craighead, Science **290**, 1532–1535 (2000).

[29] S. Sapmaz, Y. M. Blanter, L. Gurevich, and H. S. J. van der Zant, Phys. Rev. B **67**, 235414 (2003).

[30] H. J. Hwang and J. W. Kang, Physica E **27**, 163–175 (2005).

[31] M. P. Blencowe, Contemp. Phys. **46**, 249–264 (2005).

[32] K. L. Ekinci and M. L. Roukes, Rev. Sci. Instrum. **76**, 061101 (2005).

[33] F. M. Serry, D. Walliser, and G. J. Maclay, J. Appl. Phys. **84**, 2501–2506 (1998).

Ann. Phys. (Berlin) **526**, No. 3–4 (2014)

annalen der **physik**

Review Article

[34] E. Buks and M. L. Roukes, Phys. Rev. B **63**, 033402 (2001).

[35] Z. Yapu, Acta Mech. Sinica **19**, 1–10 (2003).

[36] W. H. Lin and Y. P. Zhao, Microsyst. Technol. **11**, 80–85 (2005).

[37] G. Palasantzas and J. T. M. De Hosson, Phys. Rev. B **72**, 115426 (2005).

[38] A. Ramezani, A. Alasty, and J. Akbari, Nonlinear Anal. Hybrid Syst. **1**, 364–382 (2007).

[39] W.-H. Lin and Y.-P. Zhao, J. Phys. D: Appl. Phys. **40**, 1649–1654 (2007).

[40] M. Bordag, G. L. Klimchitskaya, U. Mohideen, and V. M. Mostepanenko, Advances in the Casimir Effect (Oxford University Press, Oxford, New York, 2009).

[41] M. Abadyan, A. Novinzadeh, and A. Kazemi, Phys. Scr. **81**, 015801 (2010).

[42] J. B. Ma, L. Jiang, and S. F. Asokanthan, Nanotechnology **21**, 505708 (2010).

[43] A. Koochi, A. S. Kazemi, Y. T. Beni, A. Yekrangi, and M. Abadyan, Physica E **43**, 625–632 (2010).

[44] H. B. Chan, V. A. Aksyuk, R. N. Kleiman, D. J. Bishop, and F. Capasso, Science **291**, 1941–1944 (2001).

[45] R. Esquivel-Sirvent, L. Reyes, and J. Bárcenas, New J. Phys. **8**, 241 (2006).

[46] O. Kenneth, I. Klich, A. Mann, and M. Revzen, Phys. Rev. Lett. **89**, 033001 (2002).

[47] E. Buks and M. L. Roukes, Nature **419**, 119–120 (2002).

[48] J. N. Munday, F. Capasso, and V. A. Parsegian, Nature **457**, 170–173 (2009).

[49] K. A. Milton, E. K. Abalo, P. Parashar, N. Pourtolami, I. Brevik, and S. Å. Ellingsen, J. Phys. A: Math. Gen. **45**, 374006 (2012).

[50] U. Leonhardt and T. G. Philbin, New J. Phys. **9**, 254 (2007).

[51] F. Capasso, J. N. Munday, D. Iannuzzi, and H. B. Chan, IEEE J. Sel. Top. Quant. **13**, 400–414 (2007).

[52] A. A. Feiler, L. Bergström, and M. W. Rutland, Langmuir **24**, 2274–2276 (2008).

[53] R. Zhao, J. Zhou, T. Koschny, E. N. Economou, and C. M. Soukoulis, Phys. Rev. Lett. **103**, 103602 (2009).

[54] N. Inui, J. Appl. Phys. **111**, 074304 (2012).

[55] M. Kardar and R. Golestanian, Rev. Mod. Phys. **71**, 1233–1245 (1999).

[56] A. I. Volokitin and B. N. J. Persson, Phys. Rev. B **74**, 205413 (2006).

[57] G. V. Dedkov and A. A. Kyasov, J. Phys.: Condens. Matter **20**, 354006 (2008).

[58] J. B. Pendry, New J. Phys. **12**, 033028 (2010).

[59] J. S. Høye and I. Brevik, Eur. Phys. J. D **66**, 149 (2012).

[60] P. Lähteenmäki, G. S. Paraoanu, J. Hassel, and P. J. Hakonen, Proc. Natl. Acad. Sci. USA **110**, 4234–4238 (2013).

[61] A. Tkatchenko, R. A. DiStasio, R. Car, and M. Scheffler, Phys. Rev. Lett. **108**, 236402 (2012).

[62] R. A. DiStasio, O. A. von Lilienfeld, and A. Tkatchenko, Proc. Natl. Acad. Sci. USA **109**, 14791–14795 (2012).

[63] J. Klimeš and A. Michaelides, J. Chem. Phys. **137**, 120901 (2012).

[64] M. Bordag, U. Mohideen, and V. M. Mostepanenko, Phys. Rep. **353**, 1–205 (2001).

[65] T. Emig, Europhys. Lett. **62**, 466–472 (2003).

[66] C. Genet, A. Lambrecht, and S. Reynaud, Eur. Phys. J. Spec. Top. **160**, 183–193 (2008).

[67] S. J. Rahi, T. Emig, N. Graham, R. L. Jaffe, and M. Kardar, Phys. Rev. D **80**, 085021 (2009).

[68] A. W. Rodriguez, F. Capasso, and S. G. Johnson, Nat. Photonics **5**, 211–221 (2011).

[69] S. G. Johnson, in Casimir Physics, edited by D. Dalvit, P. Milonni, D. Roberts, and F. da Rosa (Springer Berlin, Heidelberg, 2011), pp. 175–218.

[70] M. T. H. Reid, J. White, and S. G. Johnson, Phys. Rev. A **88**, 022514 (2013).

[71] J. E. Molloy and M. J. Padgett, Contemp. Phys. **43**, 241–258 (2002).

[72] K. C. Neuman and A. Nagy, Nat. Meth. **5**, 491–505 (2008).

[73] M. L. Juan, M. Righini, and R. Quidant, Nat. Photonics **5**, 349–356 (2011).

[74] P. H. Jones, in Encyclopedia of Optical Engineering, edited by R. G. Driggers, and A. W. Hoffman (Taylor & Francis, New York, 2013).

[75] S. K. Mohanty, J. T. Andrews, and P. K. Gupta, Opt. Express **12**, 2746–2753 (2004).

[76] D. S. Bradshaw and D. L. Andrews, Phys. Rev. A **72**, 033816 (2005).

[77] J. M. Taylor and G. D. Love, Opt. Express **17**, 15381–15389 (2009).

[78] D. Haefner, S. Sukhov, and A. Dogariu, Phys. Rev. Lett. **103**, 173602 (2009).

[79] O. Brzobohatý, T. Čižmár, V. Karásek, M. Šiler, K. Dholakia, and P. Zemánek, Opt. Express **18**, 25389–25402 (2010).

[80] K. Dholakia and P. Zemanek, Rev. Mod. Phys. **82**, 1767–1791 (2010).

[81] T. Čižmár, L. C. Dávila Romero, K. Dholakia, and D. L. Andrews, J. Phys. B: At. Mol. Opt. Phys. **43**, 102001 (2010).

[82] A. Salam, Adv. Quant. Chem. **62**, 1–34 (2011).

[83] M. Lemeshko and B. Friedrich, Mol. Phys. **110**, 1873–1881 (2012).

[84] V. Demergis and E.-L. Florin, Nano Lett. **12**, 5756–5760 (2012).

[85] S. A. Tatarkova, A. E. Carruthers, and K. Dholakia, Phys. Rev. Lett. **89**, 283901 (2002).

[86] T. Thirunamachandran, Mol. Phys. **40**, 393–399 (1980).

[87] C. D. Mellor, T. A. Fennerty, and C. D. Bain, Opt. Express **14**, 10079–10088 (2006).

[88] C. Zhang, L. Sun, Y. Zhang, and C. Yan, J. Rare, Earth. **28**, 807–819 (2010).

[89] H. Lin, D. Chen, Y. Yu, A. Yang, and Y. Wang, Opt. Lett. **36**, 876–878 (2011).

[90] Y. Xu, X. Zhang, S. Dai, B. Fan, H. Ma, J.-l. Adam, J. Ren, and G. Chen, J. Phys. Chem. C **115**, 13056–13062 (2011).

[91] K. Deng, T. Gong, L. Hu, X. Wei, Y. Chen, and M. Yin, Opt. Express **19**, 1749–1754 (2011).

[92] H.-Q. Wang, M. Batentschuk, A. Osvet, L. Pinna, and C. J. Brabec, Adv. Mater. **23**, 2675–2680 (2011).

[93] C. H. Zhang, H. B. Liang, S. Zhang, C. M. Liu, D. J. Hou, L. Zhou, G. B. Zhang, and J. Y. Shi, J. Phys. Chem. C **116**, 15932–15937 (2012).

[94] O. A. Blackburn, M. Tropiano, T. J. Sorensen, J. Thom, A. Beeby, L. M. Bushby, D. Parker, L. S. Natrajan, and S. Faulkner, Phys. Chem. Chem. Phys. **14**, 13378–13384 (2012).

[95] S. W. Hao, G. Y. Chen, and C. H. Yang, Theranostics **3**, 331–345 (2013).

[96] L. Guo, Y. Wang, W. Zeng, L. Zhao, and L. Han, Phys. Chem. Chem. Phys. **15**, 14295–14302 (2013).

[97] D. L. Andrews and R. D. Jenkins, J. Chem. Phys. **114**, 1089–1100 (2001).

[98] B. W. van der Meer, G. Coker, and S. Y. S. Chen, Resonance Energy Transfer: Theory and Data (VCH, New York, 1994).

[99] D. L. Andrews and A. A. Demidov, Resonance Energy Transfer (Wiley, Chichester, 1999).

[100] G. D. Scholes, Annu. Rev. Phys. Chem. **54**, 57–87 (2003).

[101] D. L. Andrews, Can. J. Chem. **86**, 855–870 (2008).

[102] I. Medintz and N. Hildebrandt, FRET - Förster Resonance Energy Transfer: From Theory to Applications (Wiley-VCH, Weinheim, 2013).

[103] R. Gill, M. Zayats, and I. Willner, Angew. Chem. Int. Ed. **47**, 7602–7625 (2008).

[104] I. L. Medintz and H. Mattoussi, Phys. Chem. Chem. Phys. **11**, 17–45 (2009).

[105] W. R. Algar, M. G. Ancona, A. P. Malanoski, K. Susumu, and I. L. Medintz, ACS Nano **6**, 11044–11058 (2012).

[106] W. R. Algar, D. Wegner, A. L. Huston, J. B. Blanco-Canosa, M. H. Stewart, A. Armstrong, P. E. Dawson, N. Hildebrandt, and I. L. Medintz, J. Am. Chem. Soc. **134**, 1876–1891 (2012).

[107] K. D. Wegner, Z. Jin, S. Lindén, T. L. Jennings, and N. Hildebrandt, ACS Nano **7**, 7411–7419 (2013).

[108] D. Martín-Cano, L. Martín-Moreno, F. J. García-Vidal, and E. Moreno, Nano Lett. **10**, 3129–3134 (2010).

[109] D. Martín-Cano, A. González-Tudela, L. Martín-Moreno, F. J. García-Vidal, C. Tejedor, and E. Moreno, Phys. Rev. B **84**, 235306 (2011).

[110] H. Zheng and H. U. Baranger, Phys. Rev. Lett. **110**, 113601 (2013).

[111] C. Gonzalez-Ballestero, F. J. García-Vidal, and E. Moreno, New J. Phys. **15**, 073015 (2013).

[112] T. Kawazoe, K. Kobayashi, and M. Ohtsu, Appl. Phys. Lett. **86**, 103102 (2005).

[113] M. F. García-Parajó, J. Hernando, G. S. Mosteiro, J. P. Hoogenboom, E. M. H. P. van Dijk, and N. F. van Hulst, ChemPhysChem **6**, 819–827 (2005).

[114] D. L. Andrews, Energy Harvesting Materials (World Scientific, New Jersey, 2005).

[115] G. D. Scholes, G. R. Fleming, A. Olaya-Castro, and R. van Grondelle, Nat. Chem. **3**, 763–774 (2011).

[116] J. Zhang, M. K. R. Fischer, P. Bäuerle, and T. Goodson, J. Phys. Chem. B **117**, 4204–4215 (2012).

[117] L. A. Pachón and P. Brumer, Phys. Chem. Chem. Phys. **14**, 10094–10108 (2012).

[118] E. Collini, Chem. Soc. Rev. **42**, 4932–4947 (2013).

[119] L. Mandel and E. Wolf, Optical Coherence and Quantum Optics (Cambridge University Press, Cambridge, NY, 1995).

[120] D. L. Andrews and D. S. Bradshaw, J. Chem. Phys. **121**, 2445–2454 (2004).

[121] D. S. Bradshaw and D. L. Andrews, Chem. Phys. Lett. **430**, 191–194 (2006).

[122] D. L. Andrews, D. S. Bradshaw, R. D. Jenkins, and J. Rodríguez, Dalton Trans. 10006–10014 (2009).

[123] D. S. Bradshaw and D. L. Andrews, Polymers **3**, 2053–2077 (2011).